Cellular/Molecular

Voltage-Gated Na^+ Channel β1 Subunit-Mediated Neurite Outgrowth Requires Fyn Kinase and Contributes to Postnatal CNS Development *In Vivo*

William J. Brackenbury,[1] Tigwa H. Davis,[1] Chunling Chen,[1] Emily A. Slat,[1] Matthew J. Detrow,[1] Travis L. Dickendesher,[1] Barbara Ranscht,[2] and Lori L. Isom[1]

[1]Department of Pharmacology, University of Michigan, Ann Arbor, Michigan 48109-0632, and [2]Burnham Institute for Medical Research, La Jolla, California 92037

Voltage-gated Na^+ channel β1 subunits are multifunctional, participating in channel modulation and cell adhesion *in vitro*. We previously demonstrated that β1 promotes neurite outgrowth of cultured cerebellar granule neurons (CGNs) via homophilic adhesion. Both lipid raft-associated kinases and nonraft fibroblast growth factor (FGF) receptors are implicated in cell adhesion molecule-mediated neurite extension. In the present study, we reveal that β1-mediated neurite outgrowth is abrogated in *Fyn* and contactin (*Cntn*) null CGNs. β1 protein levels are unchanged in *Fyn* null brains, whereas levels are significantly reduced in *Cntn* null brain lysates. FGF or EGF (epidermal growth factor) receptor kinase inhibitors have no effect on β1-mediated neurite extension. These results suggest that β1-mediated neurite outgrowth occurs through a lipid raft signaling mechanism that requires the presence of both fyn kinase and contactin. *In vivo*, *Scn1b* null mice show defective CGN axon extension and fasciculation indicating that β1 plays a role in cerebellar microorganization. In addition, we find that axonal pathfinding and fasciculation are abnormal in corticospinal tracts of *Scn1b* null mice consistent with the suggestion that β1 may have widespread effects on postnatal neuronal development. These data are the first to demonstrate a cell-adhesive role for β1 *in vivo*. We conclude that voltage-gated Na^+ channel β1 subunits signal via multiple pathways on multiple timescales and play important roles in the postnatal development of the CNS.

Key words: **voltage-gated Na^+ channel; neurite outgrowth; auxiliary subunit; cell adhesion molecule; contactin; fyn kinase**

Introduction

Voltage-gated ion channels are multifunctional, regulating electrical excitability, intracellular signaling, transcriptional regulation, scaffolding, and cell adhesion (Dolmetsch, 2003; MacLean et al., 2003, 2005; Hegle et al., 2006; Kaczmarek, 2006; Levitan, 2006). Neuronal voltage-gated Na^+ channels (VGSCs) contain one pore-forming α subunit, one noncovalently associated β subunit (β1 or β3), and one covalently associated β subunit (β2 or β4) (Catterall, 2000; Meadows and Isom, 2005). β1 modulates channel kinetics, voltage dependence, and cell surface expression when expressed *in vitro* (Isom et al., 1992). *In vivo*, β1 also modulates electrical excitability: *Scn1b* null mice are ataxic and display spontaneous generalized seizures (Chen et al., 2004). Mutations in *SCN1B* result in human brain disease, including generalized epilepsy with febrile seizures plus and temporal lobe epilepsy (Wallace et al., 1998, 2002; Meadows et al., 2002; Audenaert et al., 2003; Scheffer et al., 2007). VGSC β subunits are unique among ion channel auxiliary subunits in that they also function as immunoglobulin superfamily cell adhesion molecules (IGSF-CAMs), directing VGSC insertion into the plasma membrane, interacting with other signaling proteins, and participating in adhesion *in vitro* (Isom et al., 1994; Isom and Catterall, 1996).

Increasing molecular evidence implicates VGSC β subunits as key mediators in cell adhesion. β1 and β2 interact with tenascin-C and tenascin-R influencing cell migration, and participate in homophilic cell adhesion resulting in cellular aggregation and ankyrin recruitment (Srinivasan et al., 1998; Xiao et al., 1999; Malhotra et al., 2000, 2002). Furthermore, β1 interacts heterophilically with N-cadherin, contactin, neurofascin-155, neurofascin-186, NrCAM, and VGSC β2 (Kazarinova-Noyes et al., 2001; Malhotra et al., 2004; McEwen and Isom, 2004; McEwen et al., 2004). Interactions between β1 and contactin, neurofascin-186, or β2 result in increased VGSC surface expression (Kazarinova-Noyes et al., 2001; McEwen and Isom, 2004; McEwen et al., 2004). We showed that β1 promotes neurite outgrowth from acutely dissociated cerebellar granule neurons (CGNs) via *trans*-homophilic cell adhesive interactions, and that this effect is blocked in neurons from *Scn1b* null mice (Davis et

Received June 20, 2007; revised Jan. 30, 2008; accepted Feb. 12, 2008.

This work was supported by National Institutes of Health (NIH) Grant R01MH059980, a grant from the Wilson Medical Research Foundation, and National Multiple Sclerosis Society Grant RG2882 (L.L.I.); by NIH Grant R01NS38297 and National Multiple Sclerosis Society Grant RG3567 (B.R.); by a University of Michigan Center for Organogenesis Non-Traditional Postdoctoral Fellowship (W.J.B.); and by NIH Grant F31NS43062 (T.H.D.). We acknowledge the expert technical assistance of Audrey Speelman and thank Dr. J. T. Elder for providing keratinocytes and Dr. K. Sue O'Shea for helpful discussions.

Correspondence should be addressed to Dr. Lori L. Isom, Department of Pharmacology, 1150 West Medical Center Drive, 1301 MSRB III, Ann Arbor, MI 48109-0632. E-mail: lisom@umich.edu.

T. H. Davis's present address: Department of Ophthalmology, University of California, San Francisco, San Francisco, CA 94143.

DOI:10.1523/JNEUROSCI.5446-07.2008

 0270-6474/08/283246-11$15.00/0

al., 2004). However, the signaling mechanism has not yet been elucidated.

IGSF-CAMs are known to localize to cholesterol and sphingolipid-rich membrane domains ("lipid rafts") that are rich in signaling molecules (Olive et al., 1995; Simons and Toomre, 2000; Kasahara et al., 2002; Niethammer et al., 2002; Schafer et al., 2004). β1 contains a putative palmitoylation site (McEwen et al., 2004), a common feature of raft-associated proteins, and colocalizes with known raft proteins on sucrose gradients after Lubrol-WX solubilization (Wong et al., 2005). Regulation of CAM-mediated neurite outgrowth involves signaling through the lipid raft-associated nonreceptor tyrosine kinase fyn (Beggs et al., 1994; Ignelzi et al., 1994; Kolkova et al., 2000). A second nonraft-associated signaling route via the fibroblast growth factor receptor (FGFR) is also known (Niethammer et al., 2002; Sanchez-Heras et al., 2006; Maness and Schachner, 2007). In the case of at least one IGSF-CAM, neural cell adhesion molecule 140 (NCAM-140), neurite outgrowth is proposed to occur via a mechanism that requires both raft and nonraft signaling pathways (Niethammer et al., 2002).

The aims of the present study were twofold: First, to evaluate the signaling mechanism(s) underlying β1-mediated neurite outgrowth; and second, to assess the effect(s) of the *Scn1b* null mutation on neuronal development *in vivo*. We demonstrate that β1-mediated neurite outgrowth requires the presence of contactin and fyn kinase, but FGFR- and epidermal growth factor receptor (EGFR)-mediated signaling pathways are not involved. The *Scn1b* null mutation results in neuronal pathfinding abnormalities in the cerebellum and corticospinal tract (CST). We propose that β1 functions as a CAM *in vivo*, and that mutations in *Scn1b* result in defective development of neurons in the CNS, leading to altered excitability.

Materials and Methods

Animals. Scn1b wild-type and null mice were generated and maintained as described previously, in accordance with the guidelines of the University of Michigan Committee on the Use and Care of Animals (Chen et al., 2004). Mice were bred from *Scn1b* heterozygous animals that had been repeatedly backcrossed to C57BL/6 mice for at least 15 generations, creating congenic strains. *Fyn* wild-type (B6;129SF2/J) and *Fyn* null (B6;129S7-*Fyn*$^{tm/Sor}$) mice were obtained from The Jackson Laboratory (Bar Harbor, ME). *Fyn* heterozygotes were then mated to produce litters containing wild-type, null, and heterozygous genotypes. *Cntn* wild-type and null mice were derived from a mixed line (129SVJ × C57BL/6 × Black Swiss) (Berglund et al., 1999). Animals used in each individual experiment were littermates.

Dissociation and culture of cerebellar granule neurons. Dissociation of cerebellar tissue from mice [postnatal day 10 (P10) to P12 for *Cntn* wild-type and null, P14 for all others] and neurite outgrowth assays were described previously (Davis et al., 2004). In some experiments, CGNs were grown in medium supplemented with one or more of the following agents 2 h after seeding: FGF (20 ng/ml; Sigma, St. Louis, MO), 1-*tert*-butyl-3-[6-(3,5-dimetoxy-phenyl)-2-(4-diethylamino-butylamino)-pyrido[2,3-d]pyrimidin-7-yl]-urea (PD173074) (50 nM; Pfizer Global Research, Groton, CT) (Niethammer et al., 2002), or 4-(3-chloroanilino)-6,7-dimethoxyquinazoline (AG1478) (2 μM; Calbiochem, La Jolla, CA) (Liu et al., 1999). Neurite length measurements were obtained from a minimum of 30 cells per condition, from at least three independent experiments. Data from individual experiments were combined to provide an overall mean and SEM.

Keratinocyte culture and proliferation assay. N/TERT human keratinocytes, kindly provided by Dr. J. T. Elder (Departments of Dermatology and Radiation Oncology, University of Michigan, Ann Arbor, MI) were cultured as described previously (Dickson et al., 2000). Briefly, cells were plated at a density of 5×10^3 cells/ml in keratinocyte serum-free medium (Invitrogen, Carlsbad, CA) supplemented with 0.4 mM $CaCl_2$, 30 μg/ml bovine pituitary extract, and 0.1 ng/ml EGF. Twenty-four hours after seeding, AG1478 (2 nM to 20 μM) was added to the growth medium and replaced after an additional 24 h. After treatment for 48 h, cells were resuspended by trypsinization and counted. Cell viability was assessed using trypan blue exclusion. Eight measurements were taken per condition, for two independent treatments. Data were combined to provide an overall mean and SEM.

Sucrose step gradient separation. C57BL/6 mice (P14–P16) were killed by decapitation and brains were quickly removed into 6 ml of ice-cold MES-buffered saline (24 mM MES, 0.15 M NaCl, pH 6.5) including 1% Triton X-100 with Complete protease inhibitors (Roche, Indianapolis, IN). The brain was homogenized using a Dounce, and then centrifuged at 1300 × *g* for 5 min at 4°C. The supernatant was then homogenized a second time and allowed to settle for 2–5 min on ice. The homogenate was adjusted to 40% sucrose and then 4 ml of a 30% and 3 ml of a 5% sucrose solution, respectively, were layered on top to form a linear sucrose step gradient. The preparation was centrifuged at 100,000 × *g* in a Beckman (Fullerton, CA) SW-41Ti rotor for 17–24 h at 4°C. Fractions of 550 μl each were collected and analyzed by SDS-PAGE.

Western blot. SDS-PAGE and transfer to nitrocellulose were performed as described previously (McEwen et al., 2004; Lopez-Santiago et al., 2006). The following primary antibodies were used: (1) anti-β1 antibody (1:1000) (Wong et al., 2005), (2) anti-α-tubulin antibody (1:5000; Cedarlane Laboratories, Burlington, NC), (3) anti-fyn kinase antibody (1:500; Santa Cruz Biotechnologies, Santa Cruz, CA), (4) anti-transferrin receptor antibody (1:1000; Zymed Laboratories/Invitrogen, Carlsbad, CA).

Densitometric analysis was performed using NIH ImageJ software. Signal density was normalized with respect to anti-α-tubulin antibody as a loading control/reference, for at least four repeat experiments.

Immunocytochemistry. Immunocytochemical analysis of dissociated CGNs was performed as described previously (Davis et al., 2004). Cells were labeled with anti-$\beta1_{ex}$ antibody (1:500) (Malhotra et al., 2002) followed by Alexa Fluor 488 anti-rabbit antibody (1:500; Invitrogen), and/or with anti-GAP43 antibody (1:500; Chemicon, Temecula, CA) followed by Alexa Fluor 594 anti-mouse antibody (1:500; Invitrogen).

Immunohistochemistry. P14 *Scn1b* null and wild-type littermate mice were anesthetized and perfused, and brains were postfixed and frozen as described previously (Davis et al., 2004). Coronal brain sections were cut to a thickness of 20 μm on a Leica (Nussloch, Germany) CM1850 cryostat, and then mounted on glass slides and stored at −20°C until use. Parallel fibers and descending axons were labeled using a monoclonal anti-TAG-1 antibody (1:100; Developmental Studies Hybridoma Bank, University of Iowa, IA), followed by Alexa Fluor 488 anti-mouse antibody (1:500; Invitrogen). Bromodeoxyuridine (BrdU)-incorporated cells were labeled on cerebellar sections from BrdU-injected mice using an anti-BrdU-Alexa Fluor 488- or 594-conjugated antibody (1:10; Invitrogen), followed by anti-mouse Alexa Fluor 594 secondary antibody (1:500; Invitrogen) to amplify BrdU signal intensity. Cell nuclei were counterstained with 4′,6-diamidino-2-phenylinodole (DAPI) (10 μg/ml; Sigma).

Confocal microscopy. Samples were viewed using an Olympus (Tokyo, Japan) Fluoview 500 confocal laser-scanning microscope with 10 and 100× objectives. Images (1024 × 1024 pixels) were initially processed with the Olympus Optical Fluoview software, and later exported into NIH ImageJ and/or Adobe Photoshop. For imaging of immunohistochemical sections, projections were created from confocal *Z*-series spanning 20 μm (interplanar distance, 0.5 μm).

Quantitative analysis of BrdU labeling. Scn1b null and wild-type littermates (P12) were injected intraperitoneally with 50 mg/kg BrdU and killed 48 h later (Vaillant et al., 2003). Animals used in each individual experiment were littermates. Ten images from the cerebellum were analyzed per mouse, for a total of three wild-type and three *Scn1b* null mice. Data were combined to provide an overall mean and SEM. The following measurements were made using NIH ImageJ software: (1) Thickness of BrdU-positive proliferating zone. For each image, three separate measurements were made from the pial layer (PL) to the innermost limit of BrdU labeling in the external germinal layer (EGL), using the straight line "Measure" function. (2) Thickness of total EGL. At the same positions

used in (1), three measurements were made from the PL to the innermost limit of the EGL, determined using DAPI-labeled nuclei. (3) Number of BrdU-positive cells. For each image, a 60-μm-long section of EGL was delineated using the freeform line "Measure" function, and the number of nuclei positive for both BrdU and DAPI was counted within. (4) Number of DAPI-positive cells. For the same 60-μm-long section of EGL, the number of nuclei positive for DAPI was counted to give an indication of the total number of cells in the EGL.

DiI labeling of corticospinal tracts. Scn1b wild-type and null mice (P9–P10) were anesthetized by hypothermia as described previously (Danneman and Mandrell, 1997; Coonan et al., 2001). DiI crystals of ~0.5 mm diameter were implanted into one side of the primary motor cortex, at bregma, just lateral to the midline. The skin was resealed with Vetbond (3M, St. Paul, MN), and the mice were allowed to recuperate for up to 1 h at 30°C. The mice were then returned to their cage and were observed to ensure that no significant motor or behavioral impairments occurred, and to ensure normal feeding. Six days after surgery, mice were anesthetized and perfused, and the brain and spinal cord were removed, post-fixed, and frozen as described previously (Davis et al., 2004). Brains and spinal cords were sectioned to a thickness of 50 μm. Images were captured at 10× on a Zeiss Axioplan fluorescent microscope at the University of Michigan Microscopy and Image Analysis Laboratory. Brains were studied from a total of seven wild-type and six *Scn1b* null mice.

Data analysis. Quantitative data are presented as mean and SEM, unless stated otherwise. AG1478 dose–response data were fitted using Prism 4 (GraphPad Software, San Diego, CA) to a sigmoidal dose–response equation: $y = y_{min} + (y_{max} - y_{min})/(1 + 10^{([LogIC50 - x]\cdot B)})$, where y_{min} and y_{max} are the minimum and maximum response plateaus, respectively; IC_{50} is the concentration of AG1478 for 50% inhibition of proliferation; x is the logarithm of AG1478 concentration; and B is the Hill slope. Pairwise statistical significance was determined with Student's two-tailed paired/unpaired *t* tests, as appropriate. Multiple comparisons were made using ANOVA followed by Tukey's *post hoc* analysis. Results were considered to be significant at $p < 0.05$ (*).

Results

Many of the cell-adhesive properties of VGSC β1 subunits are similar to those described for L1 family CAMs (Isom, 2002). In addition, we showed that β1 associates with N-cadherin (Malhotra et al., 2004). Thus, we chose to investigate whether the mechanism of β1-mediated neurite outgrowth is similar to that of these CAMs. A number of mechanisms for NCAM-, L1-CAM-, and N-cadherin-mediated neurite outgrowth have been proposed, with the greatest emphasis on a signaling pathway in the growth cone that requires CAM-mediated activation of FGFRs (Walsh and Doherty, 1997). An alternative, FGFR-independent, signaling pathway has been proposed that involves CAM-mediated activation of fyn kinase (Beggs et al., 1994, 1997; Panicker et al., 2003). Niethammer et al. (2002) unified these divergent views on the mechanism of NCAM-mediated neurite outgrowth by showing that distinct signaling pathways occur based on subcellular compartmentalization of NCAM-140 to lipid rafts or nonrafts in the plasma membrane. NCAM-140 in lipid rafts is proposed to act through initiation of the fyn–FAK kinase pathway, whereas NCAM-140 located in nonrafts acts via FGFR signaling. Both pathways are proposed to merge, with the ultimate activation of ERK1/2 (extracellular signal-regulated kinase 1/2) (Perron and Bixby, 1999; Niethammer et al., 2002). An essential feature of this proposed mechanism is that both pathways must be activated for NCAM-mediated neurite outgrowth to occur. With this in mind, we set out to test the hypothesis that β1 acts via a similar, dual pathway signaling mechanism.

β1-Mediated neurite outgrowth is inhibited in *Fyn* null mice

Fyn, a lipid raft-associated kinase (Wolven et al., 1997), is involved in NCAM-mediated neurite outgrowth (Beggs et al., 1994). To investigate a similar involvement of fyn kinase in the regulation of β1-mediated neurite outgrowth, acutely dissociated CGNs isolated from P14–P16 *Fyn* wild-type or null mice were grown on monolayers of control β1-expressing 1610 Chinese hamster lung (CHL) cells. β1 expression in the CHL monolayer increased the average neurite length of *Fyn* wild-type CGNs by 1.5-fold, from 48.7 ± 3.0 to 74.9 ± 4.3 μm ($p < 0.01$), whereas *Fyn* null CGNs showed no increase in average neurite length in response to β1 (Fig. 1*A*). In addition, β1 increased the neurite length distribution for *Fyn* wild-type but not null CGNs (Fig. 1*B*). This result is similar to that observed when *Scn1b* null neurons were grown on β1-transfected monolayers (Davis et al., 2004). Densitometric analysis of Western blots demonstrated that β1 protein expression was unchanged in *Fyn* null mice, suggesting that the lack of response of *Fyn* null CGNs to the β1-

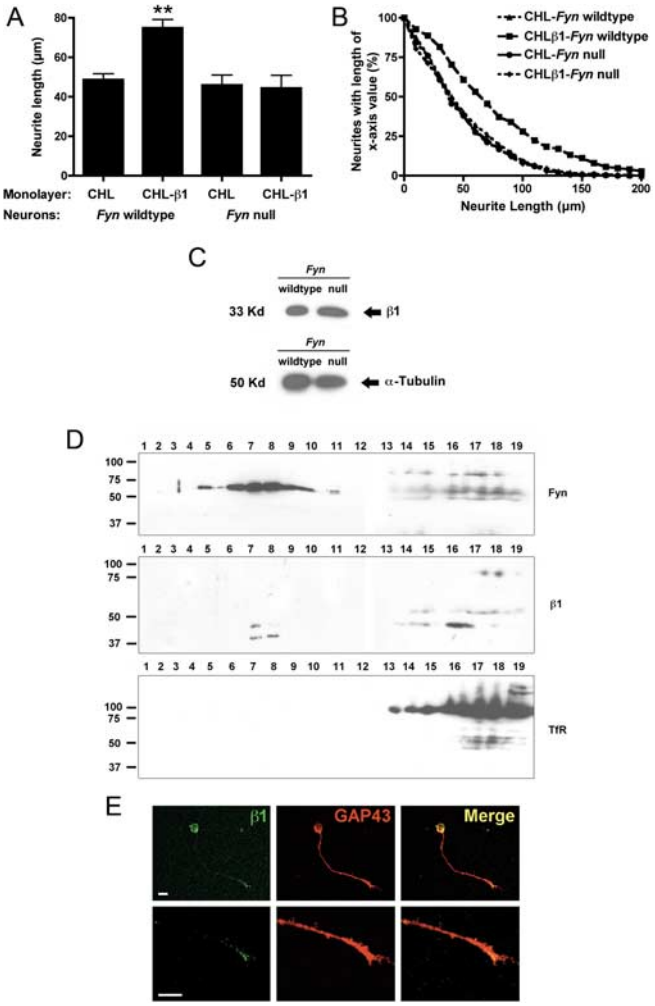

Figure 1. β1-Mediated neurite outgrowth is impaired in acutely dissociated CGNs from *Fyn* null mice. ***A***, Neurite lengths of CGNs isolated from *Fyn* wild-type and null mice grown on CHL or CHL-β1 monolayers. Data are presented as mean and SEM ($n = 250$). Significance: $^{**}p < 0.01$, ANOVA with Tukey's *post hoc* test. ***B***, Neurite distribution (in percentage) plotted against neurite length for *Fyn* wild-type and null CGNs grown on CHL or CHL-β1 monolayers. ***C***, Typical Western blot of brain membrane protein prepared from *Fyn* wild-type and null mice, using anti-β1 antibody. Anti-α-tubulin antibody was used as a control for protein loading. ***D***, Sucrose step gradient separation of protein extracted from wild-type mouse brain tissue. Blots were probed with anti-fyn kinase antibody, anti-β1 antibody, or anti-transferrin receptor (TfR) antibody. The numbers at top are gradient fractions of low-high density. Numbers at left are marker band sizes (kDa). ***E***, Images of an acutely dissociated wild-type CGN labeled with anti-$\beta1_{ex}$ (green) and GAP-43 (red) antibodies, showing β1 expression at growth cone. The bottom panels are a 3× zoom of growth cone of CGN shown in top panels. Scale bars, 5 μm.

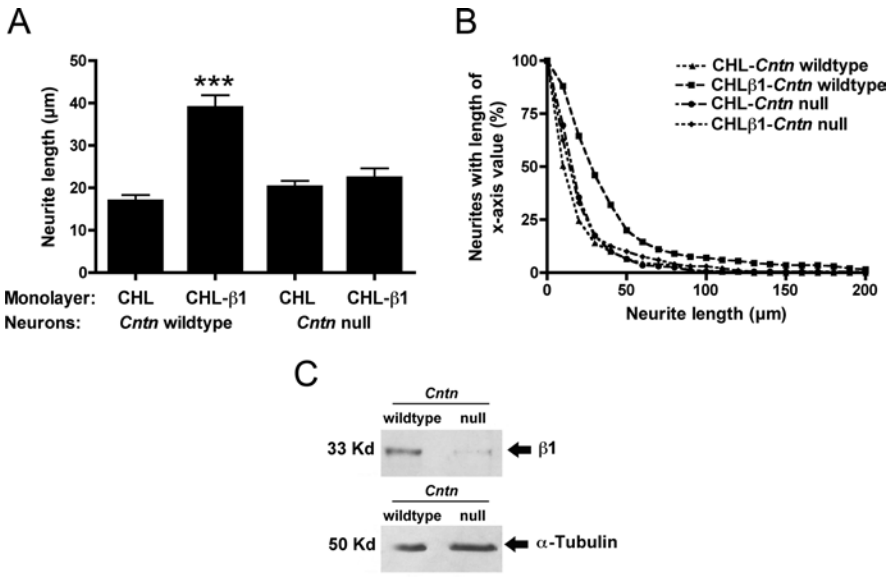

Figure 2. β1-Mediated neurite outgrowth is impaired in acutely dissociated CGNs from *Cntn* null mice. ***A***, Neurite lengths of CGNs isolated from *Cntn* wild-type and null mice grown on CHL or CHL-β1 monolayers. Data are presented as mean and SEM ($n = 200$). Significance: ***$p < 0.001$, ANOVA with Tukey's *post hoc* test. ***B***, Neurite distribution (in percentage) plotted against neurite length for *Cntn* wild-type and null CGNs grown on CHL or CHL-β1 monolayers. ***C***, Typical Western blot of brain membrane protein prepared from *Cntn* wild-type and null mice, using an anti-β1 antibody. Anti-α-tubulin antibody was used as a control for protein loading.

expressing monolayer was attributable to the loss of fyn kinase ($p = 0.41$) (Fig. 1*C*).

Both β1 and fyn kinase have been shown to localize to detergent-resistant lipid raft membrane fractions (Shenoy-Scaria et al., 1994; Kramer et al., 1999; Wong et al., 2005). To confirm that β1 and fyn kinase were indeed present in mouse brain lipid raft fractions in our hands, we isolated Triton X-100-insoluble microdomains from the brains of P14–P16 C57BL/6 mice on a sucrose step gradient. Western blot analysis revealed that fyn kinase was predominantly in low-density, Triton X-100-insoluble fractions (Fig. 1*D*). β1 protein was present in both detergent-resistant fractions with fyn kinase, and in detergent-soluble fractions with the transferrin receptor (Fig. 1*D*). Therefore, β1 may be differentially targeted within the same cell or may reside in different subcellular domains, depending on the particular neuronal or glial cell type within the brain. Immunocytochemical labeling of CGNs isolated from wild-type mice revealed that β1 subunits are localized to the growth cones (Fig. 1*E*). Together with the *Fyn* null CGN neurite outgrowth results, these data suggest that the presence of fyn kinase plays a functional role in the mechanism underlying β1-mediated neurite outgrowth in CGNs and that this signaling pathway may be initiated in lipid rafts.

β1-Mediated neurite outgrowth is inhibited in *Cntn* null mice

Contactin (*Cntn*) is a lipid raft-associated, glycophosphatidylinositol (GPI)-linked IGSF-CAM that interacts with β1 *in vitro* (Kazarinova-Noyes et al., 2001) and *in vivo* (Chen et al., 2004). Contactin and fyn kinase have been shown to coimmunoprecipitate, although likely via indirect interactions (Zisch et al., 1995). To determine whether contactin is involved in the mechanism underlying β1-mediated neurite outgrowth, acutely dissociated CGNs isolated from P10–P12 *Cntn* wild-type or null mice were grown on monolayers of control or stable, β1-expressing CHL cells, as described previously (Davis et al., 2004). β1 expression in the CHL monolayer increased the average neurite length of *Cntn* wild-type CGNs by 2.3-fold, from 16.9 ± 1.4 to 38.9 ± 2.9 μm, consistent with previous findings ($p < 0.001$) (Fig. 2*A*, left-hand bars) (Davis et al., 2004). In contrast, *Cntn* null CGNs grown on β1-transfected monolayers showed no increase in average neurite length compared with control CHL monolayers (Fig. 2*A*, right-hand bars).

The entire neurite length distribution was increased for *Cntn* wild-type CGNs grown on β1-expressing monolayers, whereas the distribution for *Cntn* null CGNs remained unchanged (Fig. 2*B*). Densitometric analysis of Western blots revealed that the β1 protein level was reduced by 73% in brain homogenates of *Cntn* null mice ($p < 0.001$) (Fig. 2*C*). The lack of response of *Cntn* null CGNs to the β1-expressing monolayer thus may result from the observed decrease in the level of β1 expression, or alternatively, contactin may play a novel functional role in the signal transduction mechanism underlying β1-mediated neurite outgrowth in CGNs.

Inhibition of FGFR and EGFR signaling does not affect β1-mediated neurite outgrowth

In hippocampal neurons, FGFR signaling is required for NCAM-dependent neurite outgrowth (Niethammer et al., 2002). To determine whether FGFR signaling is required for β1-mediated neurite outgrowth as well, CGNs were acutely dissociated from P14 C57BL/6 mice and grown on monolayers of control or stable, β1-expressing CHL cells in the presence of the FGFR tyrosine kinase inhibitor PD173074 (50 nM) for 48 h. When CGNs were grown on control CHL cell monolayers, incubation with PD173074 completely abrogated the potentiating effect of 20 ng/ml FGF on neurite outgrowth, thus confirming the activity of PD173074 (Fig. 3*A*). In the presence of carrier (DMSO) alone, β1 expression in the CHL monolayer caused an increase in average CGN neurite length of 1.8-fold, from 54.5 ± 3.3 to 95.7 ± 4.7 μm, as before ($p < 0.001$) (Fig. 3*B*, left-hand bars). Addition of PD173074 had no effect on neurite outgrowth, which still increased 1.5-fold, from 62.5 ± 2.9 to 94.2 ± 4.9 μm when β1 was stably expressed by the monolayer cells ($p < 0.001$) (Fig. 3*B*, right-hand bars).

Given that EGF has also been shown to regulate neurite outgrowth (Martinez and Gomes, 2002; Povlsen et al., 2008) and that L1-CAM-mediated cell adhesion activates EGFR tyrosine kinase (Islam et al., 2004), we next tested whether EGFR signaling is involved in β1-dependent neurite outgrowth, using the EGFR inhibitor AG1478. In a control experiment, the activity of AG1478 was confirmed by assessing its dose-dependent effect on the proliferation of N/TERT human keratinocytes. N/TERT proliferation was inhibited by 70% in the presence of 2 μM AG1478 (Fig. 3*C*), the maximum concentration at which there was no significant effect on CGN viability (data not shown). CGNs were acutely dissociated from P14 wild-type mice and grown on monolayers of control or stable, β1-expressing CHL cells in the presence of 2 μM AG1478 for 48 h. In the presence of carrier (DMSO) alone, β1 expression in the CHL monolayer caused an increase in average CGN neurite length of 1.6-fold, from 65.3 ±

3.8 to 106.4 ± 5.1 μm ($p < 0.001$) (Fig. 3*D*, left-hand bars). Addition of AG1478 had no effect on neurite outgrowth, which still increased 1.6-fold, from 63.6 ± 3.8 to 102.1 ± 5.5 μm when β1 was expressed by the monolayer cells ($p < 0.001$) (Fig. 3*D*, right-hand bars). These data show that neither FGFR activity nor EGFR activity are required for β1-induced neurite extension in CGNs.

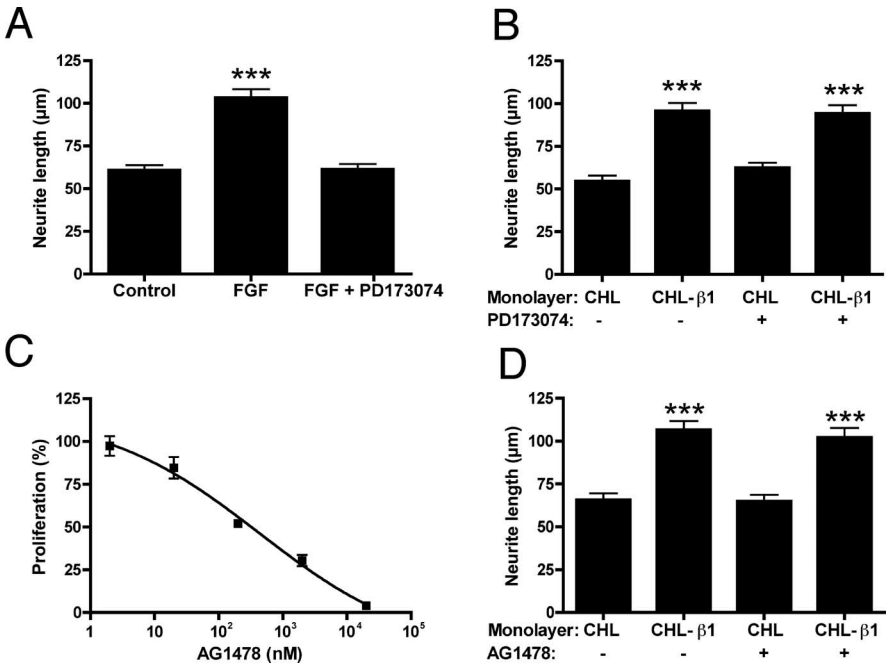

Figure 3. β1-Mediated neurite outgrowth in acutely dissociated CGNs is not affected by inhibition of EGF or FGF signaling. ***A***, Neurite length of wild-type C57BL/6 CGNs grown on CHL monolayers and treated with FGF (20 ng/ml) and/or PD173074 (50 nM) for 48 h ($n = 200$). ***B***, Neurite length of wild-type C57BL/6 CGNs grown on CHL or CHL-β1 monolayers and treated with/without PD173074 (50 nM) for 48 h ($n = 200$). ***C***, Dose-dependent inhibition of proliferation of N/TERT keratinocytes by AG1478 (2 nM to 20 μM). The line represents fit to sigmoidal function ($n = 16$). ***D***, Neurite length of wild-type C57BL/6 CGNs grown on CHL or CHL-β1 monolayers and treated with/without AG1478 (2 μM) for 48 h ($n = 250$). Data are presented as mean and SEM. Significance: ***$p < 0.001$, ANOVA with Tukey's *post hoc* test.

The *Scn1b* null mutation results in developmental defects in the cerebellum

Scn1b mice are ataxic (Chen et al., 2004), similar to *Cntn* null mice (Berglund et al., 1999) and consistent with the possibility that defects in cerebellar microorganization may have occurred as a result of the null mutation. The mouse cerebellum undergoes dramatic developmental changes during the first three postnatal weeks (Goldowitz and Hamre, 1998). In the adult, CGNs exhibit a bipolar morphology with T-shaped axons. During postnatal development, CGNs extend single axonal processes (the parallel fibers) into the deep EGL parallel to the pial surface and groups of parallel fibers subsequently become compacted into fascicles. After parallel fiber extension, CGNs attach to Bergmann glial fibers, extend a single process perpendicular to the parallel fibers, and migrate through the molecular layer (ML) to the inner granular layer (IGL) (Ramon y Cajal, 1995; Stottmann and Rivas, 1998; Berglund et al., 1999). Bergmann glia provide migrating CGNs with a substrate that is rich in CAMs, including VGSC β1, thus suggesting that β1 may play a role in outgrowth and migration of CGNs along these fibers via homophilic cell adhesion (Davis et al., 2004). To test whether β1 functions in CGN migration *in vivo*, we examined the cerebella of P14 *Scn1b* wild-type and null littermates. Cerebellar sections from *Scn1b* wild-type and null P14 littermates were labeled with an antibody to the neuronal CAM, TAG-1. TAG-1 expression is transient and restricted to CGNs during the initial stages of axon outgrowth in the EGL between P1 and P21 in rodents (Stottmann and Rivas, 1998). TAG-1 immunoreactivity has been demonstrated to be strongest on CGN cell bodies and parallel fibers and weak on radially migrating CGNs (Yamamoto et al., 1986; Furley et al., 1990; Yamamoto et al., 1990; Bailly et al., 1996). Sections were imaged first at 10×, and then three representative locations were studied at 100× (Fig. 4*A*). In both *Scn1b* wild-type and null mice, there was strong labeling of parallel fibers in the deep EGL (Fig. 4*Ai*,*ii*). In *Scn1b* wild-type mice, TAG-1-labeled parallel fibers formed tightly compacted fascicles that ran the length of the EGL, close to the interface with the ML (Fig. 4*B–D*, left-hand panels), consistent with the previously reported distribution of TAG-1 labeling in wild-type rat cerebellum (Yamasaki et al., 2001). In addition, in *Scn1b* wild-type mice, TAG-1-labeled CGN axons that descended through the ML were mostly oriented ~90° to the parallel fibers (Fig. 4*B–D*, left-hand panels). In contrast, at equivalent locations in the cerebellum of *Scn1b* null mice, the parallel fiber fascicles were less compact than those in the wild-type and in places appeared to deviate from the longitudinal axis of the EGL (Fig. 4*B–D*, right-hand panels). Although some axons descended normally through the ML, many deviated from this path. Furthermore, the TAG-1 labeling of axons descending through the ML appeared more disparate in the *Scn1b* null sections, suggesting that some axons may have turned lateral to the tissue section and exited the plane of view (Fig. 4*B–D*, right-hand panels). These migration defects were observed in all three *Scn1b* null mice studied, compared with their respective wild-type littermates.

To further study the effect of the *Scn1b* null mutation on the organization of the EGL, we performed BrdU and DAPI double-labeling (Fig. 5*A*). The outer proliferating zone (PZ) of the EGL contained the majority of BrdU-positive cells, consistent with BrdU incorporation into DNA of proliferating CGN precursors recently in S-phase (Alcaraz et al., 2006). The thickness of the PZ, defined by the lateral extent of the BrdU-positive cell nuclei, was unchanged between *Scn1b* wild-type and null mice (Fig. 5*B*, left-hand bars). In contrast, the thickness of the total EGL, measured as the lateral extent of the dense population of cell nuclei labeled with DAPI, was increased 1.4-fold in *Scn1b* null mice, from 18.7 ± 0.8 to 26.2 ± 0.9 μm ($p < 0.001$) (Fig. 5*B*, right-hand bars). We found no change in the number of BrdU-positive cells per 60-μm-long section of EGL between *Scn1b* wild-type and null mice (Fig. 5*C*, left-hand bars). However, the total number of DAPI-labeled cell nuclei per 60-μm-long section of EGL was increased 1.5-fold in *Scn1b* null mice, from 58.0 ± 2.5 to 85.1 ± 4.8 cells ($p < 0.001$) (Fig. 5*C*, right-hand bars). These results are consistent with more cells remaining in the EGL of *Scn1b* null mice compared with wild-type, without a change, either in the density of cells within the EGL, or in the absolute number of BrdU-positive, recently divided cells. Thus, the increased EGL

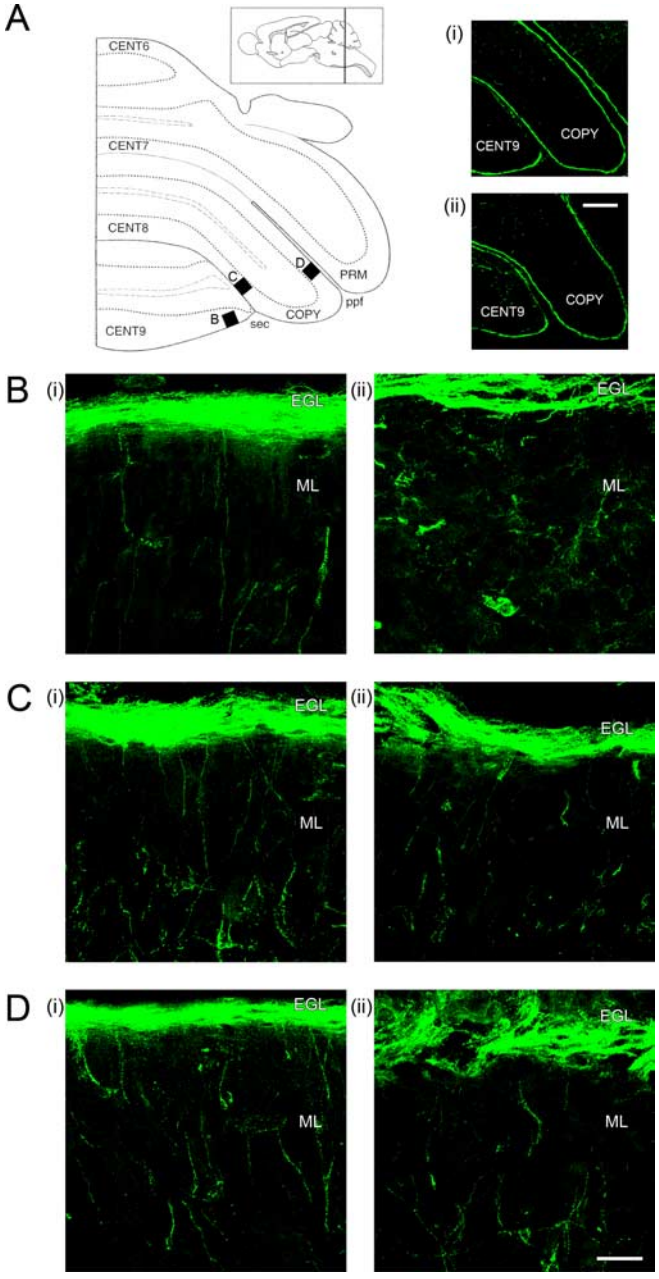

Figure 4. β1 modulates axonal migration in the postnatal developing cerebellum *in vivo*. ***A***, Schematic outline of left side of cerebellum in the coronal plane. The black boxes labeled "B–D" show locations of high-magnification images in ***B–D***. CENT6–9, Central lobe, lobules 6–9; COPY, copula pyramidis; PRM, paramedian lobule; sec, secondary fissure; prepyramidal fissure. Inset, Parasagittal diagram indicating rostrocaudal location of coronal section. ***i***, ***ii***, Right-hand plates, Low-magnification images (10×) of TAG-1 immunolabeling (green) on coronal cerebellar sections from *Scn1b* wild-type and *Scn1b* null P14 littermates, respectively. Scale bar, 100 μm. ***B–D***, High-magnification (100×) *Z*-series projections of the same *Scn1b* wild-type (***i***) and *Scn1b* null (***ii***) cerebellar sections, at the locations defined in ***A***. Scale bar, 20 μm. The schematic outline in ***A*** was adapted with permission (Hof et al., 2000). Three mice of each genotype were examined, with similar results.

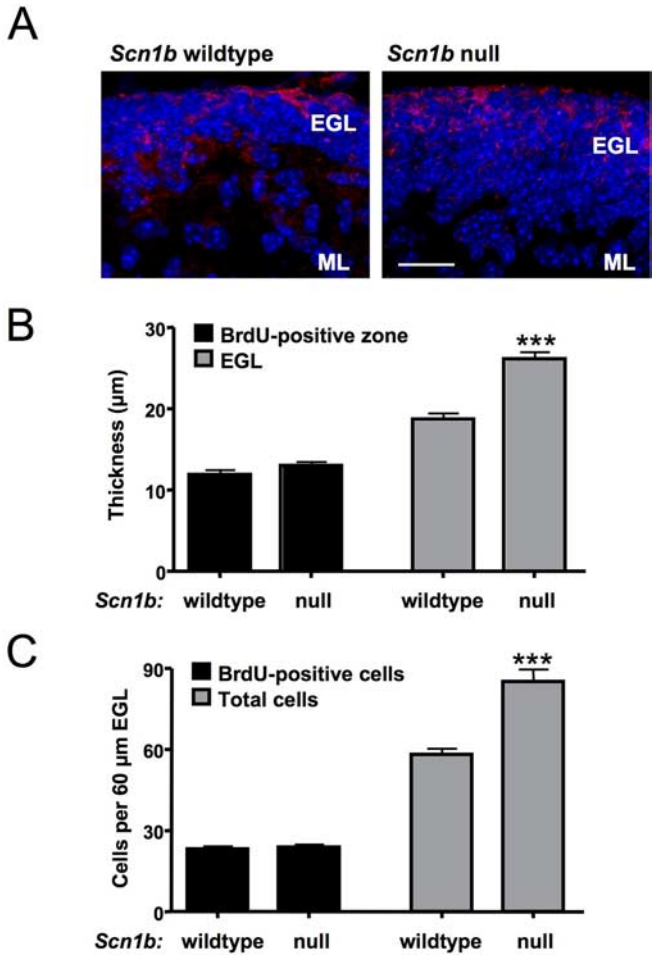

Figure 5. The external germinal layer is thicker in *Scn1b* null mice compared with wild type. ***A***, High-magnification (100×) *Z*-series projections of coronal cerebellar sections from *Scn1b* wild-type and null P14 littermates, labeled with anti-BrdU antibody (red) and DAPI (blue). Scale bar, 20 μm. ***B***, Thickness (in micrometers) of BrdU-positive zone (left-hand bars), and total EGL (right-hand bars), for *Scn1b* wild-type and null P14 littermates ($n = 90$ measurements taken from 3 mice of each genotype). ***C***, Number of BrdU-positive cells (left-hand bars), and total number of cells (right-hand bars) per 60 μm-long section of EGL, for *Scn1b* wild-type and null P14 littermates ($n = 30$ measurements taken from 3 mice of each genotype). Data are presented as mean and SEM. Significance: ***$p < 0.001$, ANOVA with Tukey's *post hoc* test.

thickness in *Scn1b* null mice is likely attributable to defective migration, rather than to a change in proliferation. Together, these data suggest that, although *Scn1b* null CGNs appear to be capable of migration, their extension of parallel fibers and subsequent descent from the EGL to the IGL along the Bergman glia fibers may be disrupted and/or delayed.

The *Scn1b* null mutation causes pathfinding defects in the CST

Our results thus far have demonstrated that CGN axonal migration and fasciculation are defective in *Scn1b* null mice. To determine whether these effects of β1 are limited to the cerebellum or whether β1 plays a more widespread role in axonal pathfinding, we examined the CST of *Scn1b* wild-type and null mice. The CST was chosen for these experiments because it is the last of the developing major fiber tracts to enter the spinal cord, coinciding with a period of β1 expression (Sutkowski and Catterall, 1990; Stanfield, 1992; Sashihara et al., 1995). In *Scn1b* wild-type mice, sequential DiI-labeled coronal sections across the pyramidal decussation confirmed normal migration of corticospinal axons from the ventral pyramid of the caudal hindbrain, across the midline, to the dorsal column of the rostral spinal cord (Fig. 6*a–g*). In contrast, in *Scn1b* null mice, we observed significant defasciculation of axons at the pyramidal decussation (Fig. 6*h–n*). Some axons began to decussate, but then turned more ventral (Fig. 6*h–l*, arrows). In addition, there was mislocalization of axons lateral to the dorsal column of the spinal cord entering into

the ventral and dorsal medullary reticular nuclei (Fig. 6*i–k*, arrowheads). Furthermore, some axons deviated from the dorsal column after the pyramidal decussation (Fig. 6*m*,*n*, arrowheads). These defects showed complete penetrance, because they were observed in all six *Scn1b* null mice studied, compared with their absence in seven wild-type littermates (additional examples from *Scn1b* null mice are in Fig. 6*o–r*).

Together, our results in the cerebellum and in the CST demonstrate a role for β1 in axonal pathfinding and fasciculation *in vivo*. We propose that β1 subunits may affect the development of late-developing fiber tracts throughout the brain via cell-adhesive interactions.

Discussion

The overall conclusions of this study are that VGSC β1-mediated neurite outgrowth is regulated by a mechanism involving fyn kinase and that β1 functions as a CAM *in vivo*. The main findings are as follows: (1) β1-mediated CGN neurite outgrowth is completely inhibited in neurons from *Fyn* null mice without a change in β1 protein level. (2) β1 protein level is significantly reduced, and β1-mediated CGN neurite outgrowth is abrogated in neurons from *Cntn* null mice. (3) In contrast to L1-family CAMs, the mechanism underlying β1-mediated neurite outgrowth does not involve signaling through EGFR or FGFR. (4) The absence of β1 results in disruption of CGN axonal pathfinding and fasciculation in the postnatal cerebellum *in vivo*. In addition, axonal pathfinding errors and decreased fasciculation were observed in the *Scn1b* null CST, suggesting that β1 may play widespread roles in the formation of late-developing neuronal tracts *in vivo*. The results of this research are novel and significant, both to the basic understanding of the dual roles of VGSC β subunits as channel modulators and as IGSF-CAMs and to the understanding of the role of β1 in human brain disease.

A lipid raft signaling mechanism for β1-mediated neurite outgrowth

Two principal signaling pathways underlying the mechanism of CAM-mediated neurite outgrowth have been identified: (1) activation of fyn kinase in lipid rafts and (2) activation of the FGFR in nonraft domains (Maness and Schachner, 2007; Ditlevsen et al., 2008). Interestingly, NCAM-140-dependent neurite outgrowth is dependent on cosignaling from both compartments (Niethammer et al., 2002). In the present study, we found that β1-mediated neurite outgrowth was completely inhibited in CGNs from *Fyn* null mice, indicating that fyn kinase is an essential component. β1 protein levels remained unchanged in *Fyn* null brains, confirming that abrogation of β1-mediated neurite outgrowth in the absence of fyn was not as a result of decreased β1 expression. The notion of fyn kinase as a signaling intermediate in CAM-mediated neurite outgrowth promotion is well es-

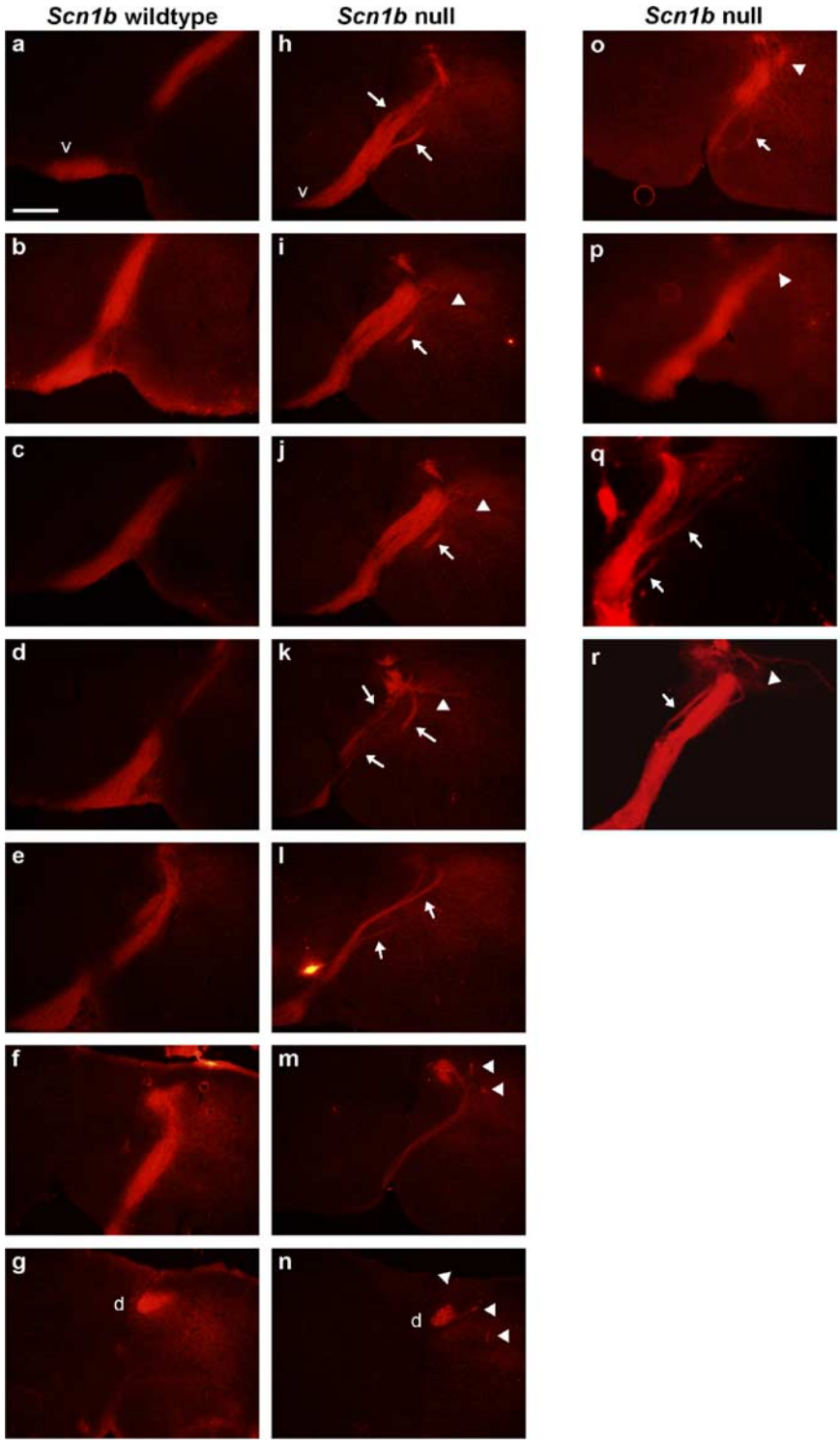

Figure 6. Loss of β1 results in axonal pathfinding abnormalities in the corticospinal tract. ***a–g***, Consecutive coronal sections across the pyramidal decussation in a *Scn1b* wild-type brain. ***h–n***, Consecutive coronal sections across the pyramidal decussation in a *Scn1b* null brain. ***o–r***, Example sections from additional *Scn1b* null mice. ***h–l***, ***o–r***, Arrows, Defasciculation across pyramidal decussation. ***i–k***, ***o–r***, Arrowheads, Mislocalization of axons lateral to dorsal column. ***m***, ***n***, Arrowheads, Axons deviating from dorsal column after pyramidal decussation. v, Ventral pyramid; d, dorsal column. Scale bar, 250 μm. Six *Scn1b* null mice were examined. All six showed similar CST abnormalities compared with seven wild-type mice.

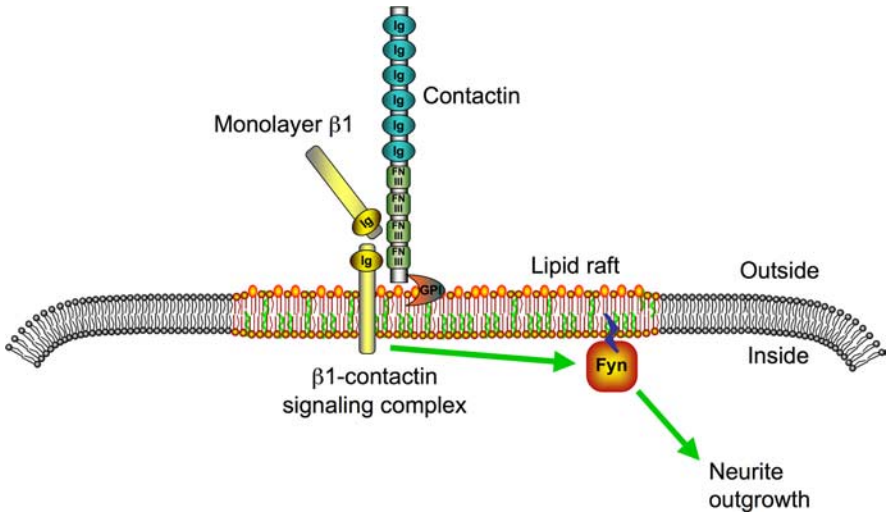

Figure 7. Schematic representation of a possible signaling mechanism underlying β1-mediated neurite outgrowth in CGNs. β1 from an adjacent cell interacts with a multiprotein complex of β1 and contactin in the CGN, initiating a signaling cascade through fyn leading to neurite outgrowth. Homophilic adhesion between β1 expressed by an adjacent cell and β1 in the CGN, and/or heterophilic adhesion between β1 expressed by an adjacent cell and contactin in the CGN may occur. Ig, Immunoglobulin domain; FN III, fibronectin type III domain. This figure was produced using Science Slides 2006 software.

tablished. For example, neurite outgrowth in response to NCAM has been is selectively inhibited in CGNs from *Fyn* null mice (Beggs et al., 1994).

β1 protein expression levels were reduced by 73% in *Cntn* null brain. Contactin expression may enhance β1 transcription and/or protein stability by unknown mechanism(s). In agreement with the latter, contactin binds to the β1 Ig loop and enhances steady-state cell surface expression of VGSC α/β subunit complexes (Kazarinova-Noyes et al., 2001; McEwen et al., 2004). Interestingly, *Cntn* null mice share some of the characteristics of *Scn1b* null mice, including ataxia, defective CGN axonal guidance, and survival only to P18 (Berglund et al., 1999). It is possible that the reduced β1 expression in *Cntn* null mice may contribute to this phenotype.

β1-Mediated neurite outgrowth was completely blocked in CGNs from *Cntn* null mice. The large reduction in β1 protein expression in the *Cntn* null may account for this abrogation. In addition, contactin may also serve alongside fyn kinase as a component of the signaling mechanism underlying β1-mediated neurite outgrowth. Previous coimmunoprecipitation studies have shown fyn and GPI-linked contactin association, presumably indirectly, via an unknown membrane-spanning molecule (Zisch et al., 1995; Kramer et al., 1999). β1 and fyn coimmunoprecipitated in Triton X-100-solubilized brain membranes in our hands; however, this result was not consistently reproducible, suggesting that these two proteins may associate transiently or with low affinity (data not shown). Binding of contactin ligands result in fyn recruitment (Zisch et al., 1995), and, at least in oligodendrocytes and contactin-transfected CHO cells, the addition of anti-contactin antibodies results in stimulation of fyn kinase (Cervello et al., 1996; Kramer et al., 1999). In oligodendrocytes, contactin-mediated fyn activation occurs specifically in rafts (Kramer et al., 1999). In addition, both β1 and fyn have been shown to interact with protein tyrosine phosphatases in brain (Zeng et al., 1999; Ratcliffe et al., 2000), providing a potential dynamic transduction capability to this signaling complex. Our results suggest that β1 may serve as a key transmembrane signaling molecule linking extracellular contactin-related cell adhesive interactions to intracellular fyn kinase, regulation of tyrosine phosphorylation, and neurite outgrowth.

In agreement with previous findings, we found that β1 and fyn were both present in detergent-resistant membrane fractions (Shenoy-Scaria et al., 1994; Kramer et al., 1999; Wong et al., 2005). Consistent with these observations, β1 contains a putative palmitoylation site juxtaposed to the inner membrane leaflet (McEwen et al., 2004), a modification commonly found in lipid raft-associated proteins, including myelin P_o, an IGSF-CAM that is closely related to β1 (McCormick et al., 1998; Pike, 2004). In addition, β1 interacts with multiple raft-associated proteins, including NrCAM, neurofascin-155, and contactin (Kazarinova-Noyes et al., 2001; McEwen and Isom, 2004; Schafer et al., 2004). Finally, β1 is modified by the raft-associated proteins γ-secretase and BACE1 (Vetrivel et al., 2005; Wong et al., 2005). Together, these findings suggest that localization of β1 to lipid rafts may be a key component in the regulation of β1-mediated neurite outgrowth (Davis et al., 2004) and that mutations affecting this localization may result in detrimental neurological effects *in vivo*.

Pharmacological blockade of either EGFR or FGFR signaling did not affect β1-mediated neurite outgrowth. We therefore conclude that the mechanism underlying β1-mediated neurite outgrowth is lipid raft-associated and requires fyn kinase. In contrast, activation of (nonraft) FGFR- or EGFR-mediated signaling pathway(s) is not involved. Based on our data, we propose that β1 expressed on the monolayer, or on an opposing neuronal or glial cell in brain, initiates a signaling cascade in the CGN via *trans* homophilic adhesion with neuronal β1 subunits, leading to neurite outgrowth (Fig. 7). The simplest scenario would involve a *cis*-β1-contactin multiprotein signaling complex providing a novel *trans* binding site(s) for β1 expressed on adjacent cells, resulting in the subsequent initiation of the fyn kinase pathway and downstream signaling cascades. β1-β1 *trans* homophilic adhesion would activate contactin via *cis*-heterophilic adhesion. In support of this, the fibronectin III domain of contactin has previously been shown to interact heterophilically with β1 (Kazarinova-Noyes et al., 2001; McEwen et al., 2004). In addition, in mouse cerebellum, contactin associates with, and transduces signaling through fyn kinase (Olive et al., 1995; Cervello et al., 1996). Alternatively, or in addition, *trans* heterophilic adhesion may occur between β1 expressed by the adjacent cell and contactin expressed by the neuron, with neuronal β1 acting as the intermediary between contactin and fyn activation. In agreement with this, β1 contains a conserved phosphotyrosine motif (Y181) in its C terminus, which is predicted to be capable of interaction with nonreceptor tyrosine kinases, such as src, fyn, or yes (Malhotra et al., 2004). Substitution of a glutamate residue, mimicking phosphorylation of Y181, abrogates recruitment of ankyrin by β1 *in vitro* (Malhotra et al., 2002; Nagaraj and Hortsch, 2006). Finally, the model is complicated by the observation that contactin may additionally affect β1-mediated neurite outgrowth indirectly, via regulating levels of surface β1 expression. Future studies will be necessary to elucidate these possibilities, and to

evaluate the possible involvement of the VGSC α-subunits in the signaling mechanism.

β1 is essential for normal CNS development

During the first 2–3 weeks of postnatal development, the CNS undergoes a period of neuronal migration and formation of synaptic connections (Singh, 1977; Amaral and Dent, 1981; Callaway and Katz, 1990). VGSC β1 subunits are expressed within this critical developmental period. For example, in rats, β1 mRNA is expressed in the hippocampus and spinal cord as early as P2, and β1 protein is expressed in the forebrain as early as P1 (Sutkowski and Catterall, 1990; Sashihara et al., 1995). In the cerebellum, β1-labeled cells in the EGL and the deep cerebellar nuclei are detected from P1 (Sashihara et al., 1995). Postmitotic CGNs leave the EGL and descend into the IGL during this postnatal period of β1 expression (Altman, 1972). In the present study, we found that β1 protein was localized to the growth cones of CGNs grown *in vitro*. In addition, in the cerebella of *Scn1b* null mice, there was disorganization of the parallel fibers as well as abnormal CGN axonal patterning through the ML into the IGL. Similar to the present data, *Cntn* null mice display misorientation of the parallel fibers with a slight reduction in their compaction within fascicles (Berglund et al., 1999). In contrast, in *L1cam* or *Nrcam* null mice, there was a reduction in the thickness of both the EGL and the IGL, without any alteration in the pattern of TAG-1 expression, suggesting that, unlike β1, these adhesion molecules may be important for CGN proliferation and/or cell survival, in addition to migration (Sakurai et al., 2001).

In the CST of *Scn1b* null mice, we observed reduced fasciculation at the pyramidal decussation, and axons projected laterally from the dorsal column, beyond the pyramidal decussation. As in the cerebellum, these effects of β1 on CST axonal pathfinding appear to be different from those of the L1-family CAMs. For example, in both *L1cam* and *Ncam1* null mice, many axons fail to cross the midline at the pyramidal decussation, but instead project ipsilaterally, resulting in a reduced number of CST axons at the opposite dorsal columns of the spinal cord (Cohen et al., 1997; Rolf et al., 2002). Thus, these L1-family CAMs are proposed to serve as guidance cues for developing axons. In contrast to L1-CAM and NCAM, β1 appears to modulate fasciculation between CST axons rather than play a role in growth cone guidance at the point of decussation, because all of the CST axons were observed to cross the midline at the appropriate point in *Scn1b* null mice. Together, these findings suggest that, as a CAM, β1 is important for normal development of the CNS.

In conclusion, we have shown that β1 plays a critical role in axon pathfinding and fasciculation during CNS development via a mechanism involving cell–cell adhesion and that is dependent on the presence of the lipid raft-associated kinase fyn and the IGSF-CAM contactin. We propose that, as a CAM, β1 participates in intercellular and intracellular communication at specialized neuronal subcellular domains, including axonal growth cones and points of axonal fasciculation. β1 subunits are multifunctional, participating in signal transduction, first on a millisecond timescale by modulating VGSC activity and, second, on a more prolonged timescale that involves cell adhesion, neurite outgrowth, and neuronal migration.

References

Alcaraz WA, Gold DA, Raponi E, Gent PM, Concepcion D, Hamilton BA (2006) Zfp423 controls proliferation and differentiation of neural precursors in cerebellar vermis formation. Proc Natl Acad Sci USA 103:19424–19429.

Altman J (1972) Postnatal development of the cerebellar cortex in the rat. 3. Maturation of the components of the granular layer. J Comp Neurol 145:465–513.

Amaral DG, Dent JA (1981) Development of the mossy fibers of the dentate gyrus: I. A light and electron microscopic study of the mossy fibers and their expansions. J Comp Neurol 195:51–86.

Audenaert D, Claes L, Ceulemans B, Lofgren A, Van Broeckhoven C, De Jonghe P (2003) A deletion in SCN1B is associated with febrile seizures and early-onset absence epilepsy. Neurology 61:854–856.

Bailly Y, Kyriakopoulou K, Delhaye-Bouchaud N, Mariani J, Karagogeos D (1996) Cerebellar granule cell differentiation in mutant and X-irradiated rodents revealed by the neural adhesion molecule TAG-1. J Comp Neurol 369:150–161.

Beggs HE, Soriano P, Maness PF (1994) NCAM-dependent neurite outgrowth is inhibited in neurons from Fyn-minus mice. J Cell Biol 127:825–833.

Beggs HE, Baragona SC, Hemperly JJ, Maness PF (1997) NCAM140 interacts with the focal adhesion kinase p125(fak) and the SRC-related tyrosine kinase p59(fyn). J Biol Chem 272:8310–8319.

Berglund EO, Murai KK, Fredette B, Sekerkova G, Marturano B, Weber L, Mugnaini E, Ranscht B (1999) Ataxia and abnormal cerebellar microorganization in mice with ablated contactin gene expression. Neuron 24:739–750.

Callaway EM, Katz LC (1990) Emergence and refinement of clustered horizontal connections in cat striate cortex. J Neurosci 10:1134–1153.

Catterall WA (2000) From ionic currents to molecular mechanisms: the structure and function of voltage-gated sodium channels. Neuron 26:13–25.

Cervello M, Matranga V, Durbec P, Rougon G, Gomez S (1996) The GPI-anchored adhesion molecule F3 induces tyrosine phosphorylation: involvement of the FNIII repeats. J Cell Sci 109:699–704.

Chen C, Westenbroek RE, Xu X, Edwards CA, Sorenson DR, Chen Y, McEwen DP, O'Malley HA, Bharucha V, Meadows LS, Knudsen GA, Vilaythong A, Noebels JL, Saunders TL, Scheuer T, Shrager P, Catterall WA, Isom LL (2004) Mice lacking sodium channel β1 subunits display defects in neuronal excitability, sodium channel expression, and nodal architecture. J Neurosci 24:4030–4042.

Cohen NR, Taylor JS, Scott LB, Guillery RW, Soriano P, Furley AJ (1997) Errors in corticospinal axon guidance in mice lacking the neural cell adhesion molecule L1. Curr Biol 8:26–33.

Coonan JR, Greferath U, Messenger J, Hartley L, Murphy M, Boyd AW, Dottori M, Galea MP, Bartlett PF (2001) Development and reorganization of corticospinal projections in EphA4 deficient mice. J Comp Neurol 436:248–262.

Danneman PJ, Mandrell TD (1997) Evaluation of five agents/methods for anesthesia of neonatal rats. Lab Anim Sci 47:386–395.

Davis TH, Chen C, Isom LL (2004) Sodium channel beta1 subunits promote neurite outgrowth in cerebellar granule neurons. J Biol Chem 279:51424–51432.

Dickson MA, Hahn WC, Ino Y, Ronfard V, Wu JY, Weinberg RA, Louis DN, Li FP, Rheinwald JG (2000) Human keratinocytes that express hTERT and also bypass a p16(INK4a)-enforced mechanism that limits life span become immortal yet retain normal growth and differentiation characteristics. Mol Cell Biol 20:1436–1447.

Ditlevsen DK, Povlsen GK, Berezin V, Bock E (2008) NCAM-induced intracellular signaling revisited. J Neurosci Res 86:727–743.

Dolmetsch R (2003) Excitation-transcription coupling: signaling by ion channels to the nucleus. Sci STKE 2003:PE4.

Furley AJ, Morton SB, Manalo D, Karagogeos D, Dodd J, Jessell TM (1990) The axonal glycoprotein TAG-1 is an immunoglobulin superfamily member with neurite outgrowth-promoting activity. Cell 61:157–170.

Goldowitz D, Hamre K (1998) The cells and molecules that make a cerebellum. Trends Neurosci 21:375–382.

Hegle AP, Marble DD, Wilson GF (2006) A voltage-driven switch for ion-independent signaling by ether-a-go-go K^+ channels. Proc Natl Acad Sci USA 103:2886–2891.

Hof PR, Young WG, Bloom FE, Belichenko PV, Celio MR (2000) Comparative cytoarchitectonic atlas of the C57BL/6 and 129/Sv mouse brains. Amsterdam: Elsevier Science.

Ignelzi Jr MA, Miller DR, Soriano P, Maness PF (1994) Impaired neurite outgrowth of src-minus cerebellar neurons on the cell adhesion molecule L1. Neuron 12:873–884.

Islam R, Kristiansen LV, Romani S, Garcia-Alonso L, Hortsch M (2004) Activation of EGF receptor kinase by L1-mediated homophilic cell interactions. Mol Biol Cell 15:2003–2012.

Isom LL (2002) The role of sodium channels in cell adhesion. Front Biosci 7:12–23.

Isom LL, Catterall WA (1996) Na^+ channel subunits and Ig domains. Nature 383:307–308.

Isom LL, De Jongh KS, Patton DE, Reber BFX, Offord J, Charbonneau H, Walsh K, Goldin AL, Catterall WA (1992) Primary structure and functional expression of the β1 subunit of the rat brain sodium channel. Science 256:839–842.

Isom LL, De Jongh KS, Catterall WA (1994) Auxiliary subunits of voltage-gated ion channels. Neuron 12:1183–1194.

Kaczmarek LK (2006) Non-conducting functions of voltage-gated ion channels. Nat Rev Neurosci 7:761–771.

Kasahara K, Watanabe K, Kozutsumi Y, Oohira A, Yamamoto T, Sanai Y (2002) Association of GPI-anchored protein TAG-1 with src-family kinase Lyn in lipid rafts of cerebellar granule cells. Neurochem Res 27:823–829.

Kazarinova-Noyes K, Malhotra JD, McEwen DP, Mattei LN, Berglund EO, Ranscht B, Levinson SR, Schachner M, Shrager P, Isom LL, Xiao Z-C (2001) Contactin associates with Na^+ channels and increases their functional expression. J Neurosci 21:7517–7525.

Kolkova K, Novitskaya V, Pedersen N, Berezin V, Bock E (2000) Neural cell adhesion molecule-stimulated neurite outgrowth depends on activation of protein kinase C and the Ras-mitogen-activated protein kinase pathway. J Neurosci 20:2238–2246.

Kramer EM, Klein C, Koch T, Boytinck M, Trotter J (1999) Compartmentation of Fyn kinase with glycosylphosphatidylinositol-anchored molecules in oligodendrocytes facilitates kinase activation during myelination. J Biol Chem 274:29042–29049.

Levitan IB (2006) Signaling protein complexes associated with neuronal ion channels. Nat Neurosci 9:305–310.

Liu W, Akhand AA, Kato M, Yokoyama I, Miyata T, Kurokawa K, Uchida K, Nakashima I (1999) 4-Hydroxynonenal triggers an epidermal growth factor receptor-linked signal pathway for growth inhibition. J Cell Sci 112:2409–2417.

Lopez-Santiago LF, Pertin M, Morisod X, Chen C, Hong S, Wiley J, Decosterd I, Isom LL (2006) Sodium channel β2 subunits regulate tetrodotoxin-sensitive sodium channels in small dorsal root ganglion neurons and modulate the response to pain. J Neurosci 26:7984–7994.

MacLean JN, Zhang Y, Johnson BR, Harris-Warrick RM (2003) Activity-independent homeostasis in rhythmically active neurons. Neuron 37:109–120.

MacLean JN, Zhang Y, Goeritz ML, Casey R, Oliva R, Guckenheimer J, Harris-Warrick RM (2005) Activity-independent coregulation of IA and Ih in rhythmically active neurons. J Neurophysiol 94:3601–3617.

Malhotra JD, Kazen-Gillespie K, Hortsch M, Isom LL (2000) Sodium channel β subunits mediate homophilic cell adhesion and recruit ankyrin to points of cell-cell contact. J Biol Chem 275:11383–11388.

Malhotra JD, Koopmann MC, Kazen-Gillespie KA, Fettman N, Hortsch M, Isom LL (2002) Structural requirements for interaction of sodium channel β1 subunits with ankyrin. J Biol Chem 277:26681–26688.

Malhotra JD, Thyagarajan V, Chen C, Isom LL (2004) Tyrosine-phosphorylated and nonphosphorylated sodium channel beta1 subunits are differentially localized in cardiac myocytes. J Biol Chem 279:40748–40754.

Maness PF, Schachner M (2007) Neural recognition molecules of the immunoglobulin superfamily: signaling transducers of axon guidance and neuronal migration. Nat Neurosci 10:19–26.

Martinez R, Gomes FC (2002) Neuritogenesis induced by thyroid hormone-treated astrocytes is mediated by epidermal growth factor/mitogen-activated protein kinase-phosphatidylinositol 3-kinase pathways and involves modulation of extracellular matrix proteins. J Biol Chem 277:49311–49318.

McCormick KA, Isom LL, Ragsdale D, Smith D, Scheuer T, Catterall WA (1998) Molecular determinants of Na^+ channel function in the extracellular domain of the β1 subunit. J Biol Chem 273:3954–3962.

McEwen DP, Isom LL (2004) Heterophilic interactions of sodium channel beta 1 subunits with axonal and glial cell adhesion molecules. J Biol Chem 279:52744–52752.

McEwen DP, Meadows LS, Chen C, Thyagarajan V, Isom LL (2004) Sodium channel β1 subunit-mediated modulation of Nav1.2 currents and cell surface density is dependent on interactions with contactin and ankyrin. J Biol Chem 279:16044–16049.

Meadows LS, Isom LL (2005) Sodium channels as macromolecular complexes: implications for inherited arrhythmia syndromes. Cardiovasc Res 67:448–458.

Meadows LS, Malhotra J, Loukas A, Thyagarajan V, Kazen-Gillespie KA, Koopman MC, S Kriegler, Isom LL, Ragsdale DS (2002) Functional and biochemical analysis of a sodium channel β1 subunit mutation responsible for Generalized Epilepsy with Febrile Seizures Plus Type 1. J Neurosci 22:10699–10709.

Nagaraj K, Hortsch M (2006) Phosphorylation of L1-type cell-adhesion molecules—ankyrins away! Trends Biochem Sci 31:544–546.

Niethammer P, Delling M, Sytnyk V, Dityatev A, Fukami K, Schachner M (2002) Cosignaling of NCAM via lipid rafts and the FGF receptor is required for neuritogenesis. J Cell Biol 157:521–532.

Olive S, Dubois C, Schachner M, Rougon G (1995) The F3 neuronal glycosylphosphatidylinositol-linked molecule is localized to glycolipid-enriched membrane subdomains and interacts with L1 and fyn kinase in cerebellum. J Neurochem 65:2307–2317.

Panicker AK, Buhusi M, Thelen K, Maness PF (2003) Cellular signalling mechanisms of neural cell adhesion molecules. Front Biosci 8:d900–d911.

Perron JC, Bixby JL (1999) Distinct neurite outgrowth signaling pathways converge on ERK activation. Mol Cell Neurosci 13:362–378.

Pike LJ (2004) Lipid rafts: heterogeneity on the high seas. Biochem J 378:281–292.

Povlsen GK, Berezin V, Bock E (2008) Neural cell adhesion molecule-180-mediated homophilic binding induces epidermal growth factor receptor (EGFR) down-regulation and uncouples the inhibitory function of EGFR in neurite outgrowth. J Neurochem 104:624–639.

Ramon y Cajal S (1995) Histology of the nervous system of man and vertebrates (Swanson N, Swanson LW, translators). New York: Oxford UP.

Ratcliffe CF, Qu Y, McCormick KA, Tibbs VC, Dixon JE, Scheuer T, Catterall WA (2000) A sodium channel signaling complex: modulation by associated receptor protein tyrosine phosphatase β. Nat Neurosci 3:437–444.

Rolf B, Bastmeyer M, Schachner M, Bartsch U (2002) Pathfinding errors of corticospinal axons in neural cell adhesion molecule-deficient mice. J Neurosci 22:8357–8362.

Sakurai T, Lustig M, Babiarz J, Furley AJ, Tait S, Brophy PJ, Brown SA, Brown LY, Mason CA, Grumet M (2001) Overlapping functions of the cell adhesion molecules Nr-CAM and L1 in cerebellar granule cell development. J Cell Biol 154:1259–1273.

Sanchez-Heras E, Howell FV, Williams G, Doherty P (2006) The fibroblast growth factor receptor acid box is essential for interactions with N-cadherin and all of the major isoforms of neural cell adhesion molecule. J Biol Chem 281:35208–35216.

Sashihara S, Oh Y, Black JA, Waxman SG (1995) Na^+ channel β1 subunit mRNA expression in developing rat central nervous system. Mol Brain Res 34:239–250.

Schafer DP, Bansal R, Hedstrom KL, Pfeiffer SE, Rasband MN (2004) Does paranode formation and maintenance require partitioning of neurofascin 155 into lipid rafts? J Neurosci 24:3176–3185.

Scheffer IE, Harkin LA, Grinton BE, Dibbens LM, Turner SJ, Zielinski MA, Xu R, Jackson G, Adams J, Connellan M, Petrou S, Wellard RM, Briellmann RS, Wallace RH, Mulley JC, Berkovic SF (2007) Temporal lobe epilepsy and GEFS+ phenotypes associated with SCN1B mutations. Brain 130:100–109.

Shenoy-Scaria AM, Dietzen DJ, Kwong J, Link DC, Lublin DM (1994) Cysteine3 of Src family protein tyrosine kinase determines palmitoylation and localization in caveolae. J Cell Biol 126:353–363.

Simons K, Toomre D (2000) Lipid rafts and signal transduction. Nat Rev Mol Cell Biol 1:31–39.

Singh SC (1977) The development of olfactory and hippocampal pathways in the brain of the rat. Anat Embryol (Berl) 151:183–199.

Srinivasan J, Schachner M, Catterall WA (1998) Interaction of voltage-gated sodium channels with the extracellular matrix molecules tenascin-C and tenascin-R. Proc Natl Acad Sci USA 95:15753–15757.

Stanfield BB (1992) The development of the corticospinal projection. Prog Neurobiol 38:169–202.

Stottmann RW, Rivas RJ (1998) Distribution of TAG-1 and synaptophysin

in the developing cerebellar cortex: relationship to Purkinje cell dendritic development. J Comp Neurol 395:121–135.

Sutkowski EM, Catterall WA (1990) β1 Subunits of sodium channels. Studies with subunit-specific antibodies. J Biol Chem 265:12393–12399.

Vaillant C, Meissirel C, Mutin M, Belin MF, Lund LR, Thomasset N (2003) MMP-9 deficiency affects axonal outgrowth, migration, and apoptosis in the developing cerebellum. Mol Cell Neurosci 24:395–408.

Vetrivel KS, Cheng H, Kim SH, Chen Y, Barnes NY, Parent AT, Sisodia SS, Thinakaran G (2005) Spatial segregation of gamma-secretase and substrates in distinct membrane domains. J Biol Chem 280:25892–25900.

Wallace RH, Wang DW, Singh R, Scheffer IE, George Jr AL, Phillips HA, Saar K, Reis A, Johnson EW, Sutherland GR, Berkovic SF, Mulley JC (1998) Febrile seizures and generalized epilepsy associated with a mutation in the Na^+-channel beta1 subunit gene SCN1B. Nat Genet 19:366–370.

Wallace RH, Scheffer IE, Parasivam G, Barnett S, Wallace GB, Sutherland GR, Berkovic SF, Mulley JC (2002) Generalized epilepsy with febrile seizures plus: mutation of the sodium channel subunit SCN1B. Neurology 58:1426–1429.

Walsh FS, Doherty P (1997) Neural cell adhesion molecules of the immunoglobulin superfamily: role in axon growth and guidance. Annu Rev Cell Dev Biol 13:425–456.

Wolven A, Okamura H, Rosenblatt Y, Resh MD (1997) Palmitoylation of p59fyn is reversible and sufficient for plasma membrane association. Mol Biol Cell 8:1159–1173.

Wong HK, Sakurai T, Oyama F, Kaneko K, Wada K, Miyazaki H, Kurosawa M, De Strooper B, Saftig P, Nukina N (2005) Beta subunits of voltage-gated sodium channels are novel substrates of BACE1 and gamma-secretase. J Biol Chem 280:23009–23017.

Xiao Z-C, Ragsdale DS, Malhorta JD, Mattei LN, Braun PE, Schachner M, Isom LL (1999) Tenascin-R is a functional modulator of sodium channel β subunits. J Biol Chem 274:26511–26517.

Yamamoto M, Boyer AM, Crandall JE, Edwards M, Tanaka H (1986) Distribution of stage-specific neurite-associated proteins in the developing murine nervous system recognized by a monoclonal antibody. J Neurosci 6:3576–3594.

Yamamoto M, Hassinger L, Crandall JE (1990) Ultrastructural localization of stage-specific neurite-associated proteins in the developing rat cerebral and cerebellar cortices. J Neurocytol 19:619–627.

Yamasaki T, Kawaji K, Ono K, Bito H, Hirano T, Osumi N, Kengaku M (2001) Pax6 regulates granule cell polarization during parallel fiber formation in the developing cerebellum. Development 128:3133–3144.

Zeng L, D'Alessandri L, Kalousek MB, Vaughan L, Pallen CJ (1999) Protein tyrosine phosphatase alpha (PTPalpha) and contactin form a novel neuronal receptor complex linked to the intracellular tyrosine kinase fyn. J Cell Biol 147:707–714.

Zisch AH, D'Alessandri L, Amrein K, Ranscht B, Winterhalter KH, Vaughan L (1995) The glypiated neuronal cell adhesion molecule contactin/F11 complexes with src-family protein tyrosine kinase Fyn. Mol Cell Neurosci 6:263–279.